

A.A. Al-Attar 

Department of Production
Engineering and
Metallurgy, University of
Technology, Baghdad,
Iraq

Attar_uot@yahoo.com

Enhance Corrosion Resistance of T22 Alloy by Adding of La₃O₂ Nanoparticles; Condition of Oil Flow

Abstract- T22 low alloy steel is represented as one of the best alloy using to production oil pipe, patrol valves, high temperature applications. This alloy has good mechanical properties, a satisfaction corrosion resistance and acceptable thermal conductivity at nature conditions. At high pressure applications with rapid flow of a fluid stream, T22 alloy is suffered severe degradation or corrosion. Though in an attempt to reduce the damage caused by corrosion, it has been resorting to the addition of La₃O₂, that is working on created a composition phase and a protective layer of corrosion. Where they were mixing alloy elements powders with different amount of La₃O₂ nanoparticles. mixed powder was prepared by powder metallurgy PM method and using a press at compression strength 175 MPa in mold steel cylindrical shape die, mold diameter is 20 mm and a height of 100 mm, sintering process has been done at a temperature 1200 °C and using Argon gas as inert gas. X-ray diffraction examination was used to identify the phases formed and microscopic structure of samples after sintering was also examined using scanning electron microscope, Archimedes method was examined to measured density and porosity of sintered samples. The examination of erosion corrosion has used a private system and thus adopted the corrosive sea water as a medium. Erosion corrosion test results showed clearly increased corrosion resistance with increasing of La₃O₂ amount, due to existence resistance to corrosion phase. 10 vol.% of La₃O₂ nanoparticles is the best nanoadditives amount which support a good resistance to erosion corrosion.

Keywords- T22 low alloy steel, erosion corrosion resistance at a high pressure, powder metallurgy method.

How to cite this article: A.A. Al-Attar, "Enhance Corrosion Resistance of T22 Alloy by Adding of La₃O₂ Nanoparticles; Condition of Oil Flow," *Engineering and Technology Journal*, Vol. 35, Part A, No. 9, pp. 936-942, 2017.

1. Introduction

The T22 steel is used to produce the boilers and oil pipes, because it is inexpensive [1], eagerly existing, simply shaped and welded to the chosen shape [2], and varied borders, are oxidation, corrosion resistant sufficient to offer acceptable service for numerous years [3]. The maximum valuable temperature is partial effect either by corrosion or by rust worries that limit the beneficial life before premature failure or changes within the microstructure happens that declines the steel much to assist in high temperature [4]. T22 Austenitic steel is exhibited in the term of the boiler tank and press the bowl symbol with two groups of allowable pressures [5]. The cause for this is its moderately low strength [6]. The uppermost permissible stress values were

determined at temperatures where use was controlled to short-term stress features [7].

Addition several elements to iron develop corrosion resistance, strength, and permanence at elevated temperature [8]. There are two elements of alloys, primitive and interplanetary. When metal atoms are like in bulk mass to iron, for example molybdenum, silicon, chromium, manganese and nickel, atoms can substitute iron at individual poetic opinions, called "*alternative solid solutions*" [9]. When minor atoms are used, for example boron, nitrogen, or carbon, lesser atoms (comparative to the size of the iron atom), substantial holes inside the matrixes are called "*solid interstitial solutions*" [10]. Carbon is by far away the utmost corporate element of alloys and has the position of both comparative to its contented [11].

Other materials are added to T22 steel enhance erosion corrosion resistance, such as Al₂O₃, SiC, MgO₂ and La₃O₂. These materials work to increase stability of created phases during works conditions [12].

High pressure powder metallurgy method is a suitable to produce T22 pipe, especially with add ceramic reinforced nanoadditives [13]. Hu Z. et. al. [14] prepared T22 by powder technology technique. They studied effect addition of Al₂O₃ nanoparticles on the fatigue behavior, the researchers observed that 4.5 vol.% of Al₂O₃ gives the best resistance. Lacroix M. et. al. [15] studied the effect of porosity content on the creep resistance at 600 °C, they obtained that little amount of porosity has a positive effect but this relation changed with high porosity.

In this work, T22 is prepared by high pressure powder metallurgy method using a uniaxial hydraulic press. La₃O₂ nanoparticles is added to this alloy and studied its effect on both porosity and erosion corrosion resistance.

2. Experimental work:

I. Prepared Green Samples

Experimentations to estimate the chemical composition of steel T22 alloy powder were performed using a rotating cylinder electrode (ECR) brand EG & G PARC Model 636 as shown in Table (1). This powder is mixed with different amount of La₃O₂ nanoparticles like Table (2) using ball mill with alumina ball media for 30 min, to insure homogenously. Polyvinyl alcohol PVA 0.5 vol.% is used as a bonding material and 0.2 vol.% of citric acid was used to disperse the aggregation of particles Mixture powder is re-blended manually for 15 min to enhance both chemical and particle size distribution. Each homologues powder batch is 5.3 gm, that compacted under uniaxial load using hydraulic press at 175 MPa. Tool-steel cylindrical die (20x100 mm) was used to prepared these green samples. Samples are ejected from die by special ejection tool.

II. Heating and Sintering Process

Electrical vacuum furnace type (Elect-MFR 23) is used to heat and sinter the green samples. Heating process is done at 650 °C for 60 min to release individual gases and violating materials. After that,

the furnace temperature is rise to reach sintering temperature 1550 °C for 120 min to ensure and enhance connections among mixture powder particles as well as reduce the porosity percentage which create between particles. Samples still, in the furnace until reach room temperature. Then, these samples are exited from furnace and prepared to subsequent testing and inspection stage.

3. Testing and Inspections

I. Density and Porosity

Green and apparent densities are measured for each sample sets. Green density is measured by using weight to volume formula [16]:

$$\rho_g = w_g / v_g$$

where w_g ; is the green sample weight, and v_g ; is the green sample volume.

Apparent density is measured using Archimedes' method in boiler fluid using the following formula [17]:

$$AD = \frac{W_d}{W_d - W_i}$$

where W_d is the dried weight, W_i is the submerged weight and W_s is the soaking weight.

Apparent porosity percentage is measured by using the below formula [18]:

$$AP = \frac{W_s - W_d}{W_s - W_i}$$

II. X-ray diffraction and SEM imaging

Identified the crystalline phases by X-ray diffraction (XRD) using a SHIMADZU XRD-600 Diffracto-meter, with monotone CuK α radiation. The applied power and current were 40.0 kV and 30.0 mA, correspondingly. The finding is generally from 10 ° to 80 ° with a phase size of 0.02 ° and a speed of 1.2 °/min. The size of sample for XRD study was 3mm × 3mm × 3mm. The microstructure of sintered samples was resolute via a Hitachi S-570 SEM, and different areas were

randomly selected in each sintered sample. SEM sample sizes were 5mm × 3mm × 3mm.

III. Erosion Corrosion Test

The medium was selected contained of a combination (o/w) deionized water to 3 vol. % NaCl, inorganic oil (0.86 g/cm³) as a supernumerary for crude. In each trial test, the oil was addition next the steel was absorbed in the NaCl solution with N₂ and soaked with CO₂ for half an hour, to evade any intrusion of the oil phase in interaction with the surface of the employed electrode. The working rod was always situated at the similar space from the border area. The metal coupons were hidden in the oil surroundings for a maximum of 30 days. The assessment of the corrosion occurrence was estimated at temperatures of 60 °C, speeds of 2000 and 5000 rpm. Erosion corrosion resistance tests were done with weight loss method. Corrosion amount rate was calculated supercilious even corrosion above the whole surface of the coupons. The corrosion rate in weight loss per area (mg/cm²) was calculated from the weight loss using the method [19]:

$$Cr\% = \frac{w}{DA t} k$$

Where; **w** = weight damage lose in grams; **k** = constant (22,300); **D** = metal density in g/cm³; **A** = coupon area (cm²); and **t** = time (days).

4. Results and Discussion

Figure (1) shows green density of pre-sintered sample sets. It is clear, that the values of green density decrease with the addition of La₃O₂ nanoparticles, possibly because of the low density of nanoparticles.

The figure (2) shows the relationships between the apparent densities, porosity with the amount of La₃O₂ nanoparticle. The inverse relationship between porosity and apparent density is clear. Decreased apparent density values for green density were observed due to the drying process

occurring during sintering process. Apparent density values increase with the increase amount of nanoparticles up to 10 vol.%, after there is a slight decrease in these values due to the conglomeration that occurred with the high amounts of the addition of nanoparticles.

Porosity values begin to decrease to 10 vol.%, then a sudden increase occurs, as a result of the closure of pores between large granules by nanoparticles. However, in large quantities, there is a conglomeration of nanoparticles that break down when fogging and thus become other pores.

Figure (3) indicate the relationship between weight loss and La₃O₂ nanoparticles with liquid speed. Weight loss values of erosion corrosion testing using two liquid speeds, first at 2000 r.p.m and the second at 5000 r.p.m. At the two speeds, the weight loss rate was reduced with the addition of nanoparticles to 10 vol.%, due to the formation of the (Fe- La₃O₂) (card no. # 04-004-2852) Figure (4) solid phase which strengthens the alloy and increase its resistance to erosion corrosion. Then increasing is done due to increased porosity caused by the aggregation of the nanoparticles. Further increases the amount of weight loss with increased fluid flow velocity, as a result of increasing the strength of erosion and removal of the material surface with increased flow velocity.

Figure (5) shows the microstructure of samples suffered erosion corrosion of all sample sets. It is observed the dimples which occur due to extraction process during corrosion test.

5. Conclusion

La₃O₂ nano-additive is created Fe- La₃O₂ hard and stable phase when added to T22 steel alloy. This phase give a high resistance to erosion corrosion condition. 10 vol.% of Fe- La₃O₂ is a best amount that support a best resistance to erosion corrosion to oil liquid.

Acknowledgment

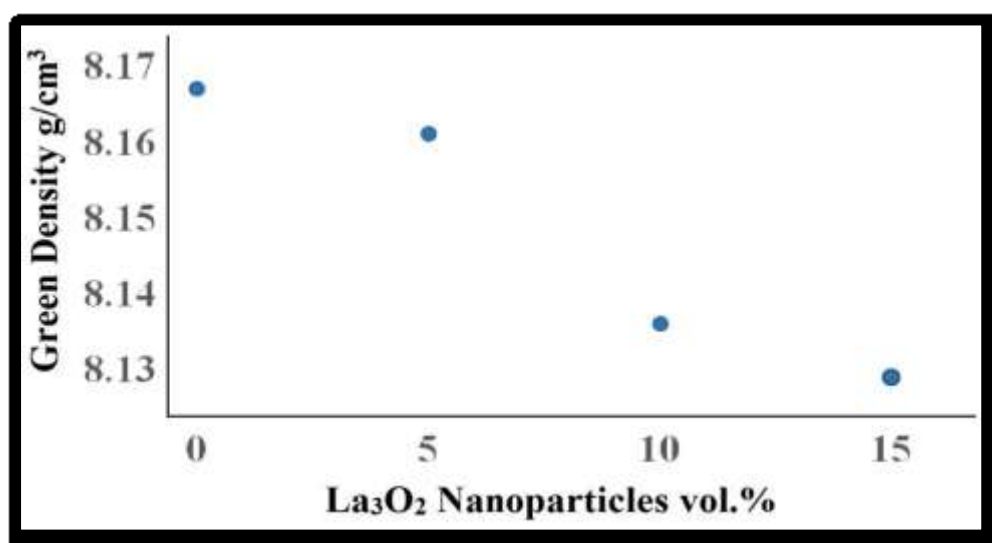
Aqeel A. Al-Attar would like to thank Dr. Clarissa Wisner for assistance in getting the SEM, and Dr. Yew San Hor for erosion corrosion weight loss capacities. The XRD results were taken in the Central Services Laboratory of Ibn Al-Haytham College in Baghdad.

Table 1: Chemical composition of T22 according to ASTM (ECR) brand EG & G PARC.

Element	C	Mn	P	S	Si	Cr	Mo
Wt.%	0.15	0.6	0.025	0.025	0.5	2	1.13

Table 2: Sample sets with different amount of La_3O_2 nanoparticles.

Sample Set	La_3O_2 nanoparticles vol.%
1	zero
2	5
3	10
4	15

Figure 1: Green density values with La_3O_2 nanoparticles vol.%.

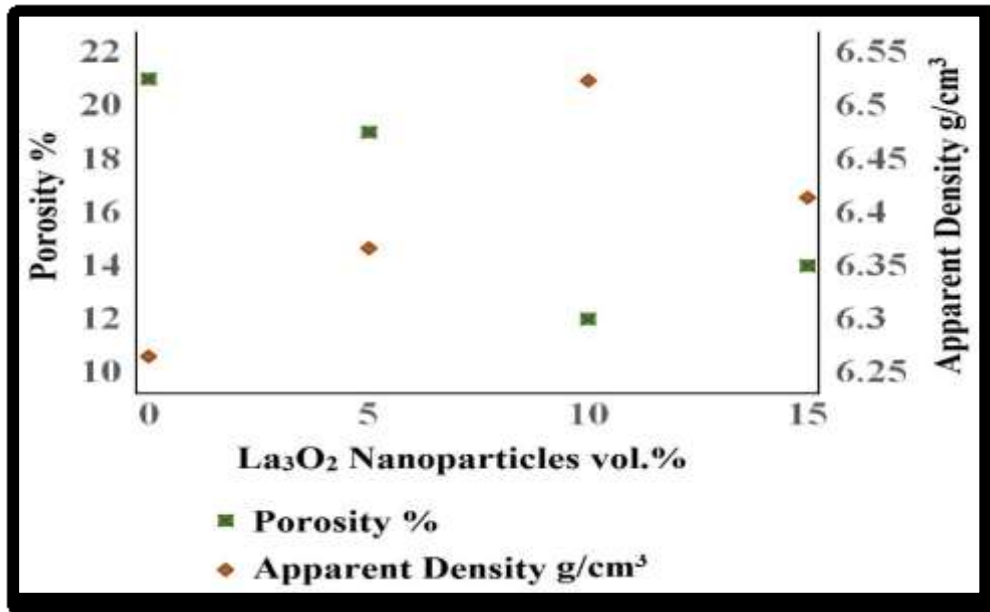


Figure 2: Apparent density and porosity values with La₃O₂ nanoparticles vol.%.

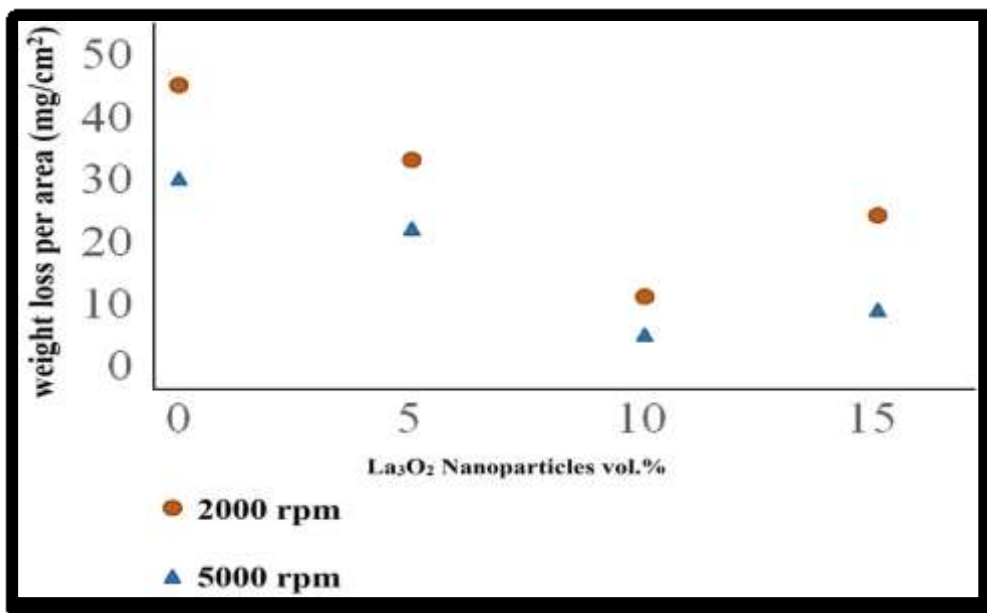


Figure 3: relationships of weight loss (mg/m²) and liquid speed with different amount of La₃O₂ nanoparticles.

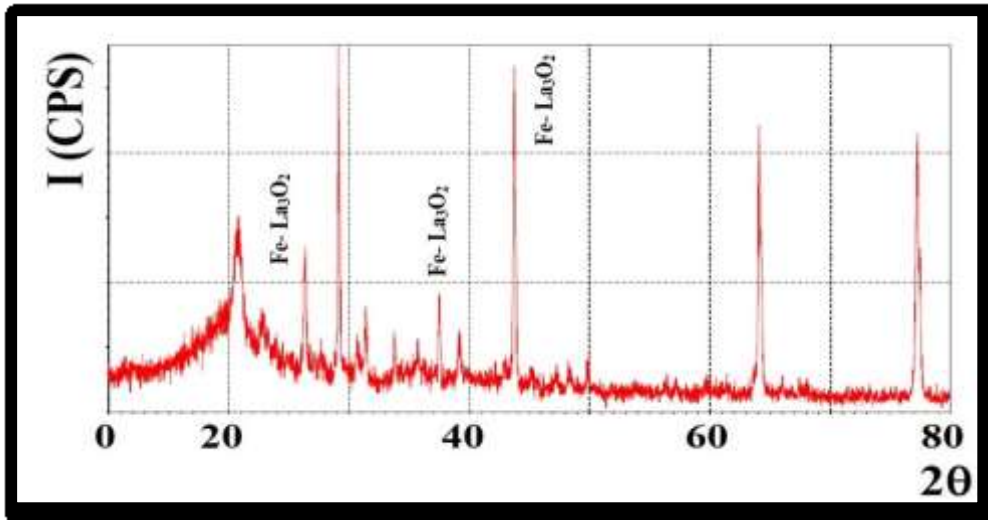


Figure 4: X-ray diffraction of sintered sample with 10 vol.% of La_3O_2 nanoparticles.

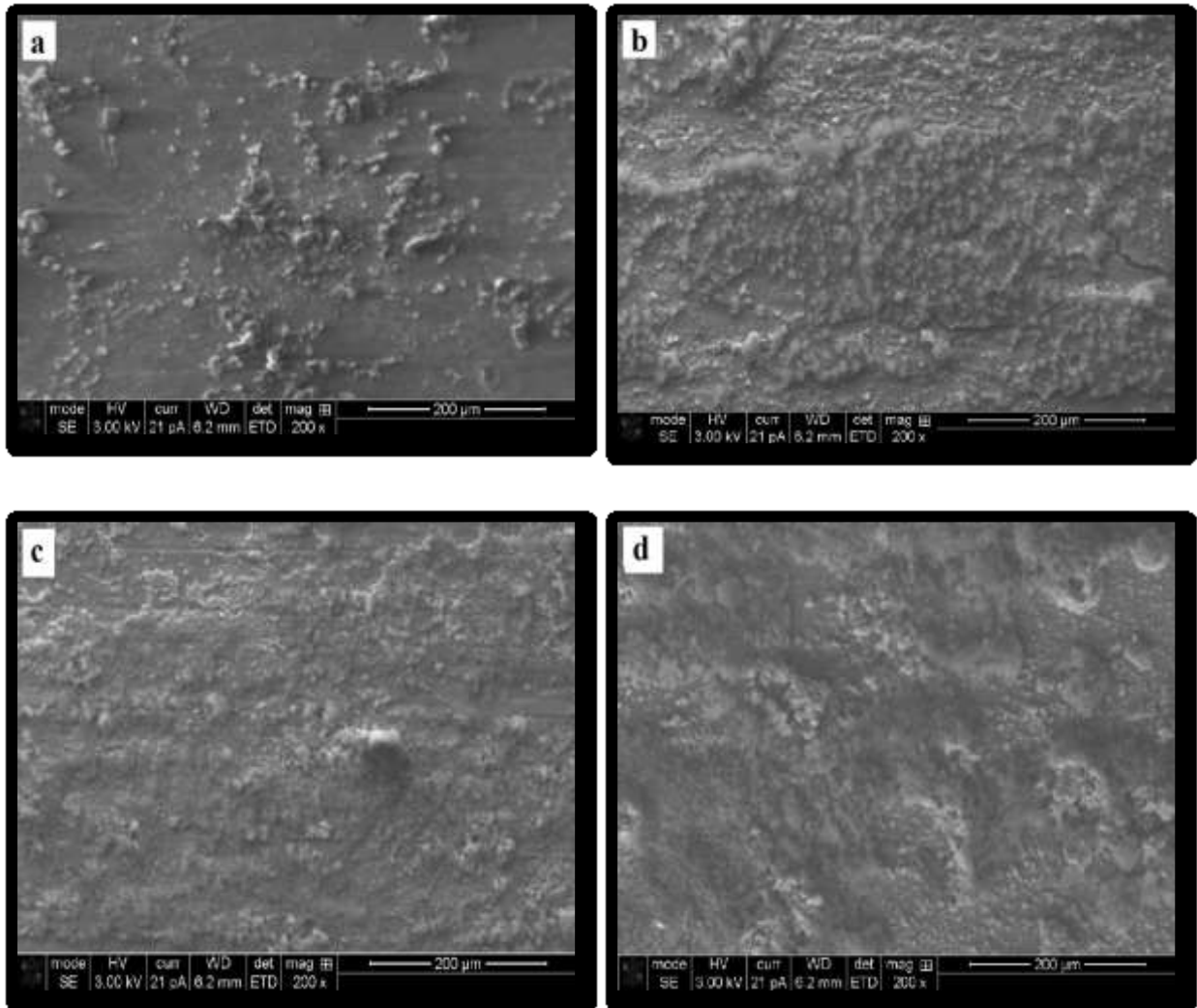


Figure 5: Microstructure of samples sets after erosion corrosion test; a) zero vol.% of La_3O_2 nanoparticles; b) 5 vol.% of La_3O_2 nanoparticles; c) 10 vol.% of La_3O_2 nanoparticles; d) 15 vol.% of La_3O_2 nanoparticles

References

- [1] Clavel Maqueda M, et al. 2011 Estudio del Proceso de Corrosión de Acero al Carbono en una Solución Tipo NACE ID196 en Presencia de Hidrocarburo XXVI Congreso de la Sociedad Mexicana de Electroquímica 4th Meeting of the Mexican Section ECS (México: Sociedad Mexicana de Electroquímica) pp 1-6
- [2] González Y.; Pineda Y.; Vera E. 2009 Mediciones EIS para Monitoreo de la Corrosión Bajo Condiciones de Flujo Multifásico Revista Latinoamericana de Metalurgia y Materiales S1(1) 298-304
- [3] Efrid K D Y, Jasinski R J 2011 Effect of the Crude Oil on Corrosion of Steel in Crude Oil/Brine Production Corrosion 45(2) 165-171
- [4] Quiroga H; Retamoso C, Macdonald D 2010 The corrosion of carbon steel in oil-in-water emulsions under controlled hydrodynamic conditions Corrosion Science 42(3) 561-575
- [5] Echeverría Félix 2015 Determinación de velocidades de corrosión en sistemas emulsionados aceite en agua (Bucaramanga: Universidad Industrial de Santander)
- [6] Farelis F; Galicia M B, Brown S 2010 Evolution of dissolution processes at the interface of carbon steel corroding in a CO₂ environment studied by EIS Corrosion Science 52(2) 509-517
- [7] Andre D, Meiler M K, Steiner Ch Wimmer 2011 Characterization of high-power lithium-ion batteries by electrochemical impedance spectroscopy I Experimental investigation, J. Power Sources, 196 5334-5341
- [8] Yadav M, Kumar S, Sinha R 2015 New pyrimidine derivatives as efficient organic inhibitors on mild steel corrosion in acidic medium: electrochemical, SEM, EDX, AFM and DFT studies Journal of Molecular Liquids 211(3) 135-145
- [9] Song G, Bowles A.L, Stjohn D H 2014 Corrosion resistance of aged die cast magnesium alloy AZ91D Materials Science and Engineering A. 366(1) 74-86
- [10] Nestic S, Brown B 2015 Corrosion under scale forming conditions Corrosion NACE International 05626 1-29
- [11] Schmitt G, Horstemeir M 2016 Fundamental aspects of CO₂ Metal Loss Corrosion-Part II: Influence of Different Parameters on CO₂ Corrosion Mechanisms NACE International Corrosion Conference Series San Diego
- [12] Forero A B, Núñez M G, Bott I S 2014 Analysis of the Corrosion Scales Formed on API 5L X70 and X80 Steel Pipe in Presence of CO₂ Materials Research 17(2) 461-471
- [13] Seuba J, Deville S, Guizard C 2016 Scientific Reports. Mechanical properties and failure behavior of unidirectional porous materials. 6(1) 2-11
- [14] Hu Z, Lu K. 2014 Evolution of pores and tortuosity during sintering. J. Am. Ceram. Soc. (97) 2383-2386
- [15] Lacroix M, Nguyen P, Schweich D, 2016 Pressure drop measurements and modeling on SiC foams. Chem. Eng. Sci. 62:3259-3267
- [16] Comiti J, Renaud M. 2015 A new model for determining mean structure parameters of fixed beds from pressure drop measurements: application to beds packed with parallelepipedal particles. Chem. Eng. Sci. 44 1539-1545
- [17] Moreira EA, Innocentini MDM, Coury JR. 2014 Permeability of ceramic foams to compressible and incompressible flow. J. Eur. Ceram. Soc. 24 3209-3218
- [18] Innocentini MDM, Salvini VR, Macedo A, 2014 Prediction of ceramic foams permeability using Ergun equation. Mater. Res. 2 283-289
- [19] Edouard D, Lacroix M, Huu CP 2010 Pressure drop modeling on SOLID foam: state-of-the art correlation. Chem. Eng. J. 144 299-311